Displacement Fields of Wood in Tension Based on Image Processing:
Part 1. Tension Parallel- and Perpendicular-to-Grain and Comparisons with Isotropic Behaviour

S. Samarasinghe and G.D. Kulasiri

Samarasinghe, S. & Kulasiri, G.D. 2000. Displacement fields of wood in tension based on image processing: Part 1. Tension parallel- and perpendicular-to-grain and comparisons with isotropic behaviour. Silva Fennica 34(3): 251–259.

Displacement fields for tensile loaded rubber and wood in parallel- and perpendicular-to-grain were obtained from digital image correlation. The results showed that the digital image correlation can reveal fine details of the nature of displacements in both rubber and wood. It was found that when load is perpendicular-to-grain, the lignin matrix produces uniform displacement fields similar to that of isotropic rubber. Uniform displacement fields also observed when lignin is involved in contraction due to Poisson effect in parallel-to-grain tension. However, when tracheids carry the load in parallel-to-grain loading, or are compressed in perpendicular-to-grain loading, a complex displacement pattern distorted by internal shear stress and slippage is produced.

Keywords deformation profiles, image processing, micro-structure, wood
Authors´ address Lincoln University, Appl. Computing, Mathematics and Statistics Group, P.O. Box 84, Canterbury, New Zealand
E-mail kulasird@tui.lincoln.ac.nz
Received 19 October 1999 **Accepted** 23 August 2000

1 Introduction

Analysis of the behaviour of wood is based on the theories and assumptions for homogeneous isotropic or orthotropic materials. However, wood is a highly variable heterogeneous material and the effect of such variable structure on mechanical properties is well recognised. Due to the lack of appropriate instrumentation, detailed studies of structural influence on mechanical behaviour of wood are very limited. Recently digital image correlation has become a useful tool for obtaining full field displacement and strain profiles in materials including wood. The method has been successfully applied to determine displacements and gradients of steel and aluminium with sub-

pixel accuracy (Chu et al. 1985). Several investigators have applied it to study compression behaviour of small wood specimens (Zink et al. 1995, Choi et al. 1991, 1996) and bolted wood joints (Stelmokas et al. 1997). In this investigation, digital image correlation is used to study in detail the tensile behaviour of wood.

1.1 Objectives

The goal of this research is to understand mechanisms of load transfer in wood in tension using digital image correlation and compare wood behaviour with that of isotropic rubber. Specifically full field displacement profiles are studied for tension parallel-to-grain, tension perpendicular-to-grain, and industrial rubber in tension to conduct a detailed assessment of the nature of the displacement characteristics in these modes of loading and to compare the three patterns of behaviour.

2 Background

Choi et al. (1991) studied parallel-to-grain compression behaviour of very small wood samples of $1 \times 1 \times 4$ mm and tensile behaviour of very small paper board samples of 5×20 mm. For wood they obtained strain parallel- and perpendicular-to-loading in an area of 0.63×2.58 mm for several load levels. The most notable feature of their strain profiles was that there was a considerable variation in strain throughout the area analysed for a constant load level. For example, strain in the load direction varied from 0.76 % to –1.0 % where positive values indicate tension showing that some areas within a compression specimen undergo tension in the direction of load. Strain perpendicular-to-loading also showed high variation ranging from –1.26 % to 1.12 % for a constant load level. Such variations indicate a significant influence of wood structure on strain fields in small specimens. For paper board, there was variation in strain but the scatter was much less compared to wood. In a paper published later in 1996, Choi et al. graphically presented contours of these highly variable strains for wood and showed that strains become concentrated near rays closer to the edge of a compression specimen. With further increase in loading these areas of strain concentration become large resulting in a failure zone associated with an area around a ray. The authors state that failure was due to stress concentrations near rays and buckling of fibres associated with these rays.

Zink et al. (1995) showed a similar phenomenon as that described above for larger wood specimens under compression parallel-to-grain loading. They compared strains in aluminium and wood blocks of dimensions $25.4 \times 25.4 \times 101.6$ mm tested in compression. They found very uniform strains throughout the surface of aluminium but highly variable strains in wood. For example, range of strain for aluminium for a particular load was 1800–2000 μstrain, whereas for wood strain varied within a much broader range between 1250–2950 μstrain. They also found that the strain in wood varied along the length as well as across the specimen. Another interesting observation was that in some areas strain perpendicular to load was greater than that in the direction of load which raises serious questions about the accepted notion of Poisson ratio. Zink et al. (1995) further state that the local areas of strain concentrations develop at load levels even below the proportional limit confirming the similar observations made for much smaller specimens by Choi et al. (1991, 1996). The observations made by these investigators point to the fact that wood behaviour is extremely complex and that full field displacement patterns can help identify mechanisms of load transfer and cause of failure in wood.

Most of the past work related to full field displacement measurements has been in compression parallel-to-grain and bending. In our study, the focus is on tensile behaviour, knowledge of which is particularly important in wood fracture studies.

3 Tensile Testing and Image Capture

Timber specimens were cut from kiln-dried flat sawn New Zealand radiata pine boards obtained from a local sawmill in Christchurch, New Zealand. Boards were kept in the laboratory for several months before they were cut into 10 specimens with dimensions 180×95 mm $\times$ 10 mm for each category. The loading plane for wood specimens was Longitudinal-Tangential (LT) with the thickness in radial direction. Moisture content of the specimens at the time of testing was approximately 12 %, average density was 390 kg/m^3, and average Young's modulus was 8.0 GPa. Medium flexibility industrial rubber was obtained from a local shop and dimensions of the two rubber specimens were $95 \times 60 \times 4$ mm. The Youngs's modulus of the rubber specimens were tested experimentally and found to be 3.167 MPa. From the elastic theory, shear modulus is 1.267 MPa for a Poisson ratio of 0.25.

Tests were conducted on a computer controlled SINTECH material testing workstation. Special tensile jigs were manufactured to hold the specimens in the jaws and a schematic of the test setup with equipment used to capture images are shown in Fig. 1. Specimens were speckled with black and white paint to obtain a random speckle pattern as required for image processing and illuminated by a fibre optic ring light level of which could be controlled. This allowed a very uniform level of illumination throughout the surface. Images were captured by an Ikigami CCD (Charge Couple Device) video camera with 25 frames per second capture rate. Images were digitized to 512×512 pixels by a high accuracy 8 bit monochrome CX100 frame grabber/digitizer on an IBM 486DX66 computer. Live analogue video signal was shown on a black and white analogue monitor and the digitized image was shown on the computer monitor.

Tests were conducted at a rate of 2 mm/min and the software that drives the testing machine provided a load-time curve, which was used to capture images at various load levels. Generally, 2 to 5 images were captured in each test. Prior to testing, a graph paper was placed against the specimen surface and its image was captured to calibrate the image distances to real distances. The resolution for the current setup was 54 pixels/cm in the horizontal and 83 pixels/cm in the vertical directions.

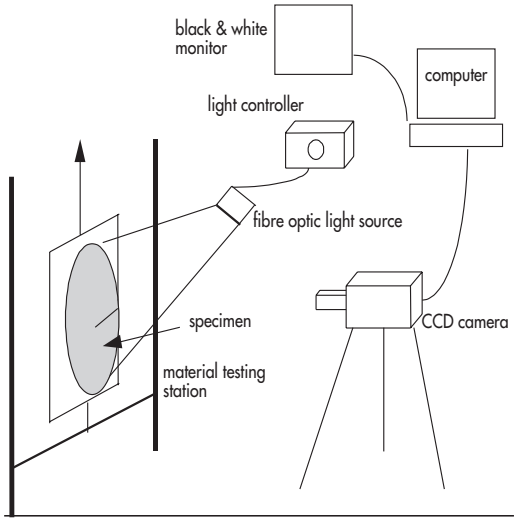

Fig. 1. Schematic diagram of the test set-up and image capture.

3.1 Image Processing

Digital Image Correlation (DIC) is a non-contacting full-field strain measuring technique for obtaining full field surface displacements and their gradients (strains) of objects under stress. The DIC method has evolved over the last decade and vast improvements have been made to the efficiency and reliability of computations. Theory of digital image correlation has been described by many researches (Bruck et al. 1989, Chu et al. 1985, Sutton et al. 1988, 1986, 1983, Peters et al. 1983). The underlying principle of DIC is that points on the undeformed surface can be tracked to new positions on the deformed image using an error minimisation technique. To achieve this, the object surface must have a random light intensity pattern that makes a small area surrounding a point unique and able to be tracked. For each point of interest, a small subset surrounding the point is chosen in the undeformed image and the subset in the deformed image

that is the closest in light intensity to the original subset is sought based on linear elastic displacement theory in conjunction with grey level intensity of points in the image. This is an iterative process that requires an appropriate choice of parameter values to be optimized and an error estimation procedure. In the program used in this study (Vic-2D, 1998), Newton Raphson method and statistical cross-correlation are used in the analysis. To initiate the search process, known initial vertical and horizontal displacements of a point in the image is specified. Then the program computes displacements for any number of specified points.

An area of 20 cm^2 as shown in Fig. 2 was selected for analysis and displacements for points located at 1.85 mm intervals horizontally and 1.2 mm vertically were obtained. Thus for a particular pair of images, displacements of about 900 points were determined. The focus of this paper is on horizontal and vertical displacements, and results for a representative specimen are presented for each category of tests.

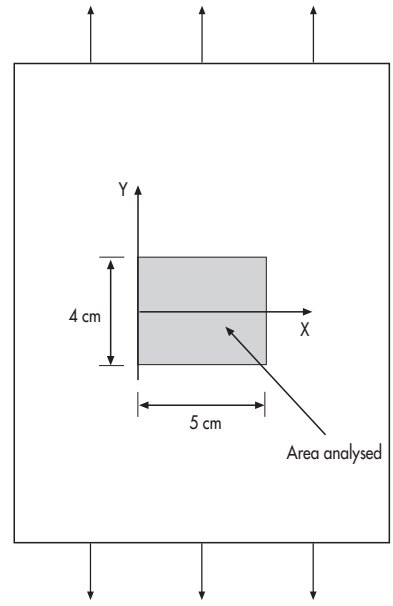

Fig. 2. Co-ordinate system and location of the analyzed area.

4 Results and Discussion

4.1 Notation of the Coordinate Axes

Coordinate axes for all specimens are defined in such a way that x axis coincides with the centre line of the area analyzed, y axis with the left border of the same area, and the material point at the origin of the coordinate system is fixed so that its displacement is zero (Fig. 2). This means that the movement of all points is measured with respect to the fixed point located at the origin. This was done mainly to eliminate any rigid body motion from the measured displacements. The data obtained from digital image correlation underwent a major transformation to conform to this format. This data processing and subsequent plotting was done using Mathematica 3.0 (Wolfram Research 1997).

4.2 Deformation in an Isotropic Rubber Plate

The purpose of this analysis was to ascertain the level of detail that can be seen from a displacement profile obtained from digital image correlation for a homogeneous isotropic material and to use it for comparison with results obtained for wood plates. Area analyzed was 5.5 × 3.6 cm (Fig. 2) and constituted about 25 % of the total specimen area.

4.2.1 Vertical Displacement (v)

The vertical displacement is that in the direction of y-axis as shown in Fig. 2. Fig. 3 (a) shows the 3-Dimensional (3-D) plot of the vertical displacement (v) for the area analyzed and Fig. 3 (b) displays the same profile in contour form for a load of 3 N. The 3-D plot shows that the points with positive y co-ordinates move in the positive direction and those with negative y co-ordinates move in the opposite direction symmetrically as expected. Contour plot shows fairly horizontal bands of iso-displacement contours indicating

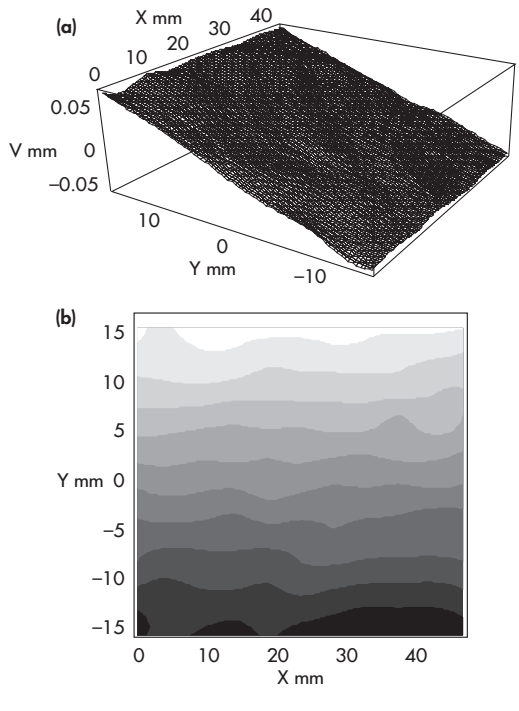

Fig. 3. Vertical displacement profiles in rubber. (a) Three-Dimensional (3-D) profile and (b) contour plot.

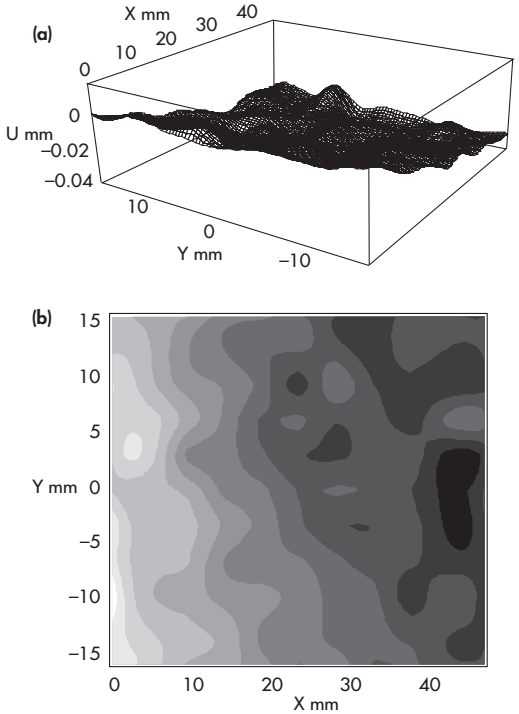

Fig. 4. Horizontal displacement profiles in rubber. (a) 3-D profile and (b) contour plot.

that points with identical y coordinates deform similar magnitude. Profile shown is exactly what is expected. A closer observation of the 3-D plot shows ripples propagating parallel to the diagonal (45° to the y-axis). The pattern seems to reveal the influence of shear as maximum shear force in a tensile specimen is in a plane inclined 45° to the principle axis (load axis in this case).

4.2.2 Horizontal Displacement (u)

Horizontal displacement is that in the direction of x-axis as shown in Fig. 2. When a plate is stretched, it contracts in the horizontal direction. For a fixed origin, therefore, maximum contraction must be on the border opposite the origin with the displacement decreasing towards the origin. The 3-D plot in Fig. 4 (a) shows a contraction that is uniformly decreasing towards the origin confirming the expected behaviour. The displacement contours in Fig. 4(b) further reveals that they are not perfect vertical bands but somewhat distorted. This may be due to the influence of shear which is more prominent here than for the v displacement profile. Comparison of Figs. 3(a) and 4(a) indicates that v and u displacements maintain a Poisson ratio of 0.3 to 0.4.

In summary, it can be stated that v and u profiles show expected patterns and magnitudes of displacements very well. They also show variations to the expected behaviour showing how a real material that is assumed to be perfectly isotropic and homogeneous behaves under load. There appears to be visible influence of shear which is more prominent for u displacement.

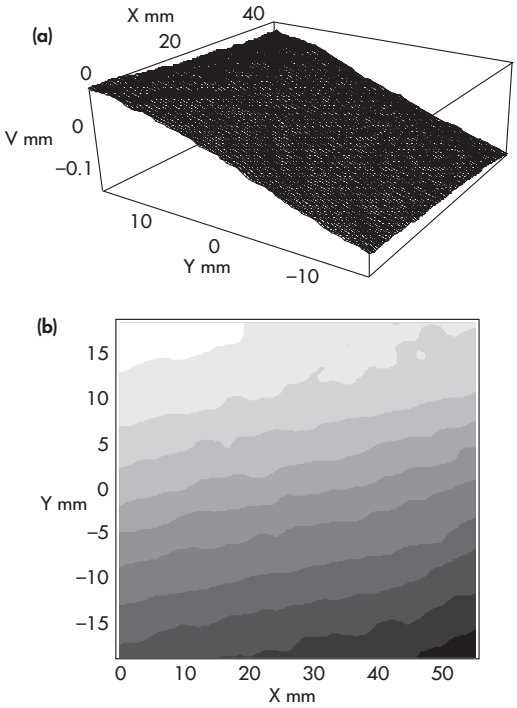

Fig. 5. Vertical displacement profiles in wood loaded perpendicular-to-grain. (a) 3-D profile and (b) contour plot.

4.3 Displacement Profiles for a Wood Plate Loaded Perpendicular-to-Grain in Tension

4.3.1 Vertical Displacement (v)

When loaded perpendicular-to-grain, the lignin matrix resists the load and tracheids only transfer the load to the matrix. Figs. 5(a) and 5(b) show 3-D and contour plots of v for the analyzed area of 5.5 cm × 3.6 cm for a 7 kN load. Note that the material point that coincides with the origin of the coordinate system is fixed so that v = 0 for this point. Plots indicate that the analysed region has undergone a total displacement roughly equal to 0.2 mm. Most notable features of this profile are its uniformity and similarity to that of rubber. However, the displacement along any plane parallel to x-axis is not constant, as was the case for rubber, as can be seen from slanted iso-displacement contours of Fig. 5(b). For rubber, contours were almost horizontal. What gives rise to the angled displacement contours in wood loaded perpendicular to the grain? The lignin matrix that resists the load being isotropic in nature cannot produce the slanted contours. One reason could be that the deformation is guided by tracheids that are not completely perpendicular to the load axis. It is almost impossible to have grain orientation collinear with x-axis in a real specimen and slight grain deviation could have affected how the lignin matrix deformed. Another reason could be that the ripple effect that appears to be due to shear is more prevalent here than for rubber and it exerted a noticeable influence on the slanted profile. It is possible that a combination of both of these influences produced the inclined profiles.

4.3.2 u Displacement

When loaded perpendicular-to-grain, horizontal u displacement is contraction along the grain. Fig. 6 (a) shows the 3-D plot of u for the area analyzed for fixed coordinates at the origin where u = 0. The total displacement in the area analyzed is close to 0.1 mm which is higher than expected in this direction compared to v displacement shown above. However, a closer examination of the displacement profile reveals reasons for the observed behaviour. The most striking feature of this profile is that it is much noisier or coarser than that for rubber which also showed some noise. Another notable feature is that instead of contraction with respect to the origin, as was the case for rubber, there is positive movement above the x axis near the top right hand area and negative movement in the bottom left hand region as if the top region is shearing non-uniformly in the x direction with respect to the bottom region thereby increasing the total displacement in the x direction. Furthermore, one would expect vertical bands in the contour plot (Fig. 6(b)) but they are almost exactly 45° to the y-axis or along the diagonal of the rectangular area. This is confirmed by the ripples in the 3-D plot that shows 45° degree slant indicating the influence of shear to a larger degree than that manifested in rubber. It appears

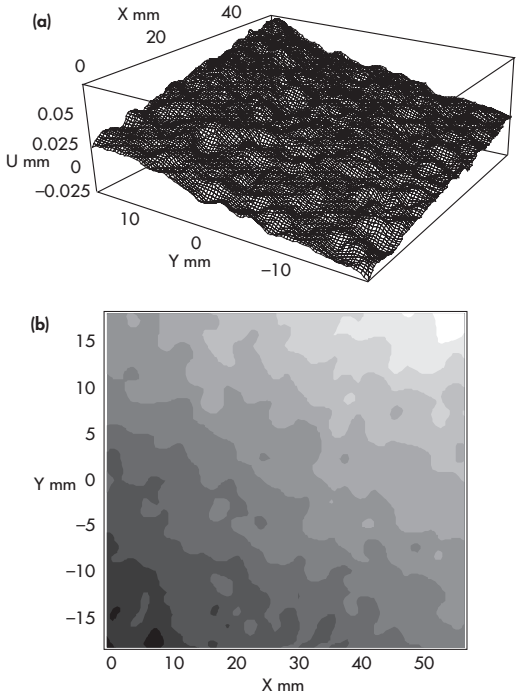

Fig. 6. Horizontal displacement profiles in wood loaded perpendicular-to-grain. (a) 3-D profile and (b) contour plot.

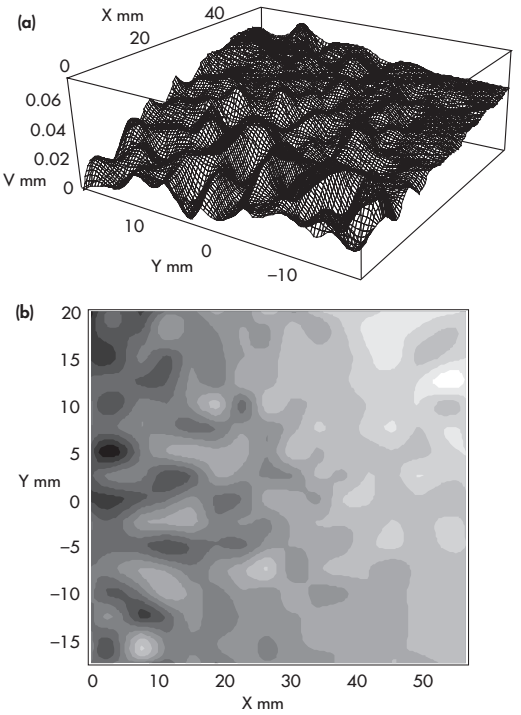

Fig. 7. Vertical displacement profiles in wood loaded parallel-to-grain. (a) 3-D profile and (b) contour plot.

that the maximum shear stress acting along a plane inclined 45° to the load axis exerts its influence on the tracheids that are being compressed causing shearing along the grain in x direction thereby producing a complex slanted displacement profile. Intuitively one could expect fibre buckling under these conditions and its effect would be to enhance the displacement. Similar effect of influence of shear is present in wood under compression where tracheids buckle under the combined influence of compression and shear.

4.4 Displacement Profiles for a Wood Plate Loaded Parallel-to-Grain in Tension

4.4.1 Vertical Displacement (v)

In this mode the load is applied parallel to the tracheids that resist the load. Fig. 7(a) and 7(b) show 3-D and contour plots of v in an area of 5.5 cm × 3.6 cm in the middle of the plate for a 10 kN load. The most striking feature here is that the displacement is not symmetric about x-axis as was the case for rubber and wood perpendicular to grain. Most of the displacement is positive in this profile which can only happen if there is predominant vertical slippage or shear between tracheids in the area analysed compared to normal stretching. This can be expected considering how tracheids are bonded together in the finger-jointed fashion. Slanted contours in the contour plot indicate another influence in addition to verti-

cal slippage which can be attributed to maximum shear stress acting at 45° to load axis. It is interesting to note the similarity in form between this profile and u displacement profile for perpendicular to grain loading (Figs. 6(a) and (b)) where contraction of tracheids due to Poisson effect is displayed. Comparison of Figs. 7 and 6 reveals a strong evidence of shear interacting with the elongation and or contraction of tracheids causing the ripple effect along planes parallel to the diagonal or 45° to the load that resulted in slanted contours in Figs. 7(b) and 6(b). This analogy points to a peculiar displacement pattern along tracheids, which is very different to that across it. When lignin matrix is involved in load transfer, it invokes a fairly uniform and symmetric extension about the x-axis (Fig. 5a); in contrast, when tracheids transfer load, some vertical slippage between tracheids produce somewhat vertical bands which are further distorted by internal shear stress. The plot indicates an overall displacement of about 0.7 mm.

4.4.2 Horizontal Displacement (u)

In parallel-to-grain loading u is a measure of contraction of the lignin matrix in the x direction. Fig. 8(a) displays a 3-D plot and 8(b) a contour plot of u for the 5.5 cm × 3.6 cm area where u(0,0) = 0. It is interesting to note how remarkably similar the u displacement profiles shown here and that for rubber given in Figs. 4(a) and 4(b). Plots show a negative u displacement, which is the highest at the right border. Why are these two plots similar? It must be because lignin matrix that is being deformed due to Poisson effect is isotropic and behaves similar to the isotropic rubber. The magnitude of the total displacement in the area is about 0.5 mm which is reasonable compared to the v displacement discussed above.

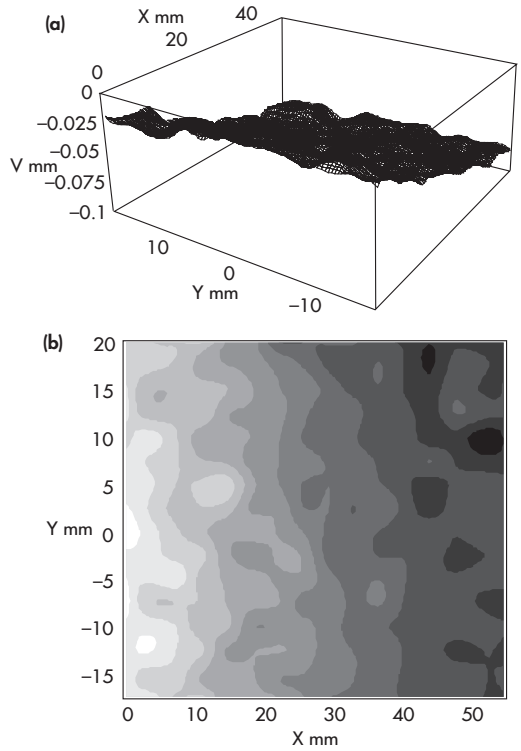

Fig. 8. Horizontal displacement profiles in wood loaded parallel-to-grain. (a) 3-D profile and (b) contour plot.

5 Summary and Conclusions

Displacement fields were obtained for rubber and wood loaded parallel- and perpendicular-to-grain in tension using digital image correlation method. The displacement profiles thus obtained revealed intricate details of the mechanisms of load transfer in isotropic rubber and anisotropic wood confirming that the digital image correlation is a useful method for detailed analysis of displacements. The study of rubber and wood members showed clearly the difference between isotropic and orthotropic behaviour. Specifically, isotropy invokes fairly uniform horizontal and vertical displacements in rubber; whereas, in wood entirely different displacement mechanisms are found for parallel- and perpendicular-to-grain. For example, when loaded perpendicular-to-grain, extension is similar to isotropic rubber

owing to uniform properties of the lignin matrix; but contraction along the tracheids is subjected to internal slippage as well as internal shear stress leading to a very complex displacement profile. Reverse behavior is found when loaded parallel-to-grain; extension profile shows slippage and internal shear whereas contraction (u) results in uniform displacement pattern similar to rubber owing to uniform nature of displacement of lignin.

References

Bruck, H.A., McNeill, S.R., Sutton, M.A. & Peters, W.H. 1989. Digital image correlation using Newton-Raphson method of partial differential correction. Experimental Mechanics (1989): 261–267.

Choi, D., Thorpe, J.L. & Hanna, R.B. 1991. Image analysis to measure strain in wood and paper. Wood Science and Technology 25: 251–262.

— , Thorpe, J.L., Cote Jr., W.A. & Hanna, R.B. 1996. Quantification of compression failure propagation in wood using digital image pattern recognition. Forest Products Journal 46(10): 87–93.

Chu, T.C., Ranson, W.F., Sutton, M.A. & Peters, W.H. 1985. Application of digital image correlation techniques to experimental mechanics. Experimental Mechanics (1985): 232–244.

Wolfram Research. 1997. Mathematica Version 3.0.

Peters, W.H., Ranson, W.F., Sutton, M.A., Chu, T.C. & Anderson, J. 1983. Application of digital correlation methods to rigid body mechanics. Optical Engineering 22(6): 738–742.

Stelmokas, J.W., Zink, A.G. & Loferski, J.R. 1997. Image correlation analysis of multiple-bolted connections. Wood and Fiber Science 29(3): 210–227.

Sutton, M.A., Wolters, W.J., Peters, W.H., Rawson, W.F. & McNeill, S.R. 1983. Determination of displacements using an improved digital image correlation method. Image and Vision Computing 1(3): 133–139.

— , Cheng, M., Peters, W.H., Chao, Y.J. & McNeill, S.R. 1986. Application of an optimized digital correlation method to planar deformation analysis. Image and Vision Computing 4(3): 143–150.

— , McNeill, S.R., Jang, J. & Babai, M. 1988. Effects of subpixel image resolution on digital correlation error estimates. Optical Engineering 27(10): 870–877.

Vic-2D. Version 2.1. 1998. Digital Image Correlation, Cimpiter, Inc. USA.

Zink, A.G, Davidson, R.W. & Hanna R.B. 1995. Strain measurement in wood using a digital image correlation technique. Wood and Fiber Science 27(4): 346–359.

Total of 13 references